Nakamura and Yamamoto *Robomech J (2017) 4:18*
DOI 10.1186/s40648-017-0085-3

ROBOMECH Journal

RESEARCH ARTICLE Open Access

Modeling and control of electroadhesion force in DC voltage

Taku Nakamura* and Akio Yamamoto

Abstract

In this paper, a new model for electroadhesion between two surface-insulated plates under DC electric field is presented and control of dynamic responses of electroadhesion force is discussed. Under DC electric field, even if the voltage difference between the plates is constant, electroadhesion force increases or decreases over time depending on the insulating materials. The increase had been explained by Johnsen–Rahbek (JR) model, but the decrease had not been focused or modeled by physically meaningful way. In addition, the previous models did not explicitly consider the mechanical behaviors of the electrodes, although the mechanical behaviors considerably affect the response. In this work, we introduced a new model that combines both electrical and mechanical behaviors. The electrical part, which is based on JR model, explained the force decrease under DC field, in addition to the force increase that had been explained using JR model. The mechanical part was represented by a combination of a spring and a damper. Numerical simulations using the model successfully reproduced characteristics behaviors of electroadhesion force, which include force decay under constant voltages and relatively smaller initial force. Using the inverse model, we carried out experiments to control dynamic responses of electroadhesion force, which successfully controlled force responses against pulse voltages. Through the experiments, we also showed the importance of the neutralization of surface charges for obtaining reproducible responses.

Keywords: Electrostatic adhesion, Bilayer dielectric, Interface charge, Johnsen–Rahbek effect, Built-in sensor, Haptic display

Background

Two surfaces having different electrical potentials stick to each other by electrostatic force, which is called *electroadhesion*. The electroadhesion has been utilized for various applications. The early application is electrostatic chucks for handling silicon wafers [1, 2] or glass substrates in IC or LCD production lines. Recently, the application areas of the electroadhesion have been expanding to robotics and haptics. In robotics field, researchers have proposed unique applications such as wall/ceiling-attachment for drones [3], soft grippers [4], and wall-climbing robots [5–9], as the electroadhesion can be realized with a simpler and lighter devices compared to other adhesion methods [5, 6, 10]. For those robotic applications, inter-digital electrodes have been preferred due to its adhesion capability to dielectric surfaces. The behavior of inter-digital electrodes in the context of electroadhesion has recently been studied extensively [8, 11, 12]. Electroadhesion has also been applied to surface haptic displays [13–18], in which electroadhesion modulates friction on a transparent electrode that covers an LCD surface, to create haptic effects. In those haptic applications, planar electrodes have been preferred, rather than inter-digital electrodes.

In these relatively new application fields, especially in the field of haptics, control of dynamic responses of electroadhesion force is required. To facilitate dynamic response control, an electric model that can describe the internal electric effect needs to be developed. In the conventional electrostatic chucks for wafer handling, electroadhesion force gradually increases under a DC voltage, which is called Johnsen–Rahbek (JR) effect. This JR effect is due to the conductivity of the surface insulators. The resulting electroadhesion force grows considerably large,

*Correspondence: taku_nkat@aml.t.u-tokyo.ac.jp
Department of Precision Engineering, The University of Tokyo, Hongo 7-3-1, Tokyo 113-8656, Japan

much larger than typical electrostatic attraction force calculated using the text-book parallel plate model. Watanabe et al. developed an electric model to describe JR effect [19], which has been extensively utilized in analyzing the conventional electrostatic chucks [20, 21].

On the other hand, studies in the field of haptics reported that their electroadhesion force decreases under a constant DC voltage applications [13, 16, 22]. In those studies, less conductive materials are used as surface insulators, whereas electrostatic chucks intentionally add some conductivity to the insulating materials. To explain the decreases, those studies tried to develop different electric models. However, although those models successfully reproduced the force decrease, they do not explain the electroadhesion phenomena in a physically meaningful way. In addition, electroadhesion often involves mechanical responses of the electrodes. Therefore, electric model alone is not enough; an electro-mechanical combined model is required for dynamic response control.

Although fast and accurate control of electroadhesion force, especially under DC voltages, is imperative in the field of haptics and robotics, it has been a challenging issue, due to the lack of reasonable models. In this paper, we propose an electro-mechanical model for electroadhesion and demonstrate dynamic control of electroadhesion force using the inverse of the proposed model. The electric part of the proposed model is based on JR model. In this work, we have analyzed the JR model developed by Watanabe to show that it can also explain the force decreases observed in haptic studies. One of the reasons that the previous studies failed to model the electroadhesion would be unstable behaviors of electroadhesion device. This paper points out that the unstable behaviors originate in the initial electric charges on the surface of the electroadhesion device. Our experiments have shown that stable behaviors are obtained by removing the initial surface charges. Finally, we have demonstrated that dynamic response of the electroadhesion can be controlled based on the proposed electro-mechanical model.

The structure of this paper is as follows. "Related work" reviews issues on modeling and control of electroadhesion. "Electroadhesion model" introduces an electro-mechanical combined model. "Control of electroadhesion" demonstrates the force control based on the model. "Discussion" denotes limitations of the model and the experiments. "Conclusion" summarizes this paper.

Related work

The simplest model for electroadhesion is the parallel-plate-capacitor model. Assuming a pair of electrodes insulated by one or more dielectrics, the model expresses electroadhesion force F_e as

$$F_e = \frac{1}{2}\varepsilon_0 A \left(\frac{V}{\hat{d}}\right)^2, \tag{1}$$

where ε_0 is the absolute permittivity of vacuum, A is the area of the electrode, and V, $\hat{d}$ are the voltage difference and the equivalent gap between the electrodes. This model is often used for simple estimation of the adhesion force [23]. However, it is only valid in a steady state of AC voltage condition. Therefore, previous studies that required electroadhesion force control often resorted to AC voltages, instead of using DC (or low frequency AC) voltages, such that they can rely on this simple model [14, 16].

Due to mechanical and electrical responses, the actual generated force changes dynamically. The mechanical response is caused by elastic deformation of asperity in surface roughness [21] and macroscopic deformation of the electrodes/insulators [17]. In the previous study, the authors showed that the mechanical responses can be compensated by estimating the equivalent gap by using a built-in sensor that measures the capacitance of the paired plates [18].

Regarding the electrical response, two different models have been mainly studied. One is leakage model [24, 25] that can explain decrease of electroadhesion force observed in haptic studies [13, 16, 22]. In the leakage model, the paired electrodes have two dielectrics and one of them has a leak resistance as shown in the equivalent circuit of Fig. 1a. By focusing on the voltage across the leakage-side dielectrics (V_2), the model can explain the force decrease. Although the model can reproduce the experimentally observed force variations, correspondence between the model and the actual setup, or the physical background of the model, remains rather unclear compared to JR model explained in the next.

The other model is JR model. Since its first report in [26], the increase of the force has been explained by charge accumulation at the borders of the microscopic air gap. When the dielectrics between the paired electrodes have conductivity, charges are accumulated and held by the gap, resulting to the force increase. This model is expressed as the equivalent circuit in Fig. 1b [19–21], which consists of an air-gap and conductive dielectric

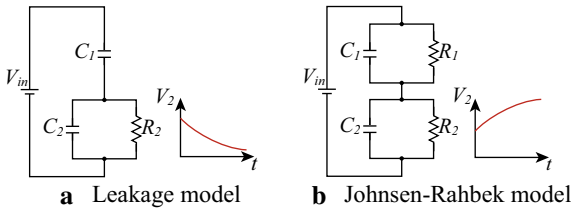

a Leakage model **b** Johnsen-Rahbek model

Fig. 1 Equivalent circuits for leakage and Johnsen–Rahbek model

layers. The air gap is also assumed to have conductivity corresponding to the contact resistance. By calculating the adhesion force from the voltage across the air gap, the model can explain the force increase. However, our observations in our previous studies indicated that the responses of electroadhesion force cannot be perfectly explained with these electrical models alone; mechanical behavior needs to be taken into account.

Electroadhesion model

Concept

In this work, we propose an electro-mechanical model for electroadhesion, with a special focus on force decreasing type. Although, the previous studies have tried to explain the force decrease by the leakage model, this work adopts JR model as it has better physical background.

In Fig. 2a, our assumption for the air gap is illustrated. A basic electroadhesion mechanism consists of a pair of surface-insulated electrodes. The insulators are a dielectric material but has a slight electrical conductivity. Between the contact surfaces, there is an air gap due to surface roughness and macroscopic deformation of the electrodes. This air gap behaves like a dielectric material having a slight electrical conductivity since charge relaxation occurs between the contact surfaces.

Based on the assumption, this work models the electroadhesion mechanism as a bilayer dielectric with electric loss as shown in Fig 2b. The two insulators on actual setups are summarized into one insulating layer in this model for simplification. The model shares the same concept with the JR model developed by Watanabe [19]. However, our model includes the mechanical aspect represented by the spring (spring constant: k) and the damper (damping constant: c), as shown in Fig 2b. To facilitate the combination with the mechanical aspect, our model focuses on electric field, E, whereas Watanabe's JR model focuses on voltages.

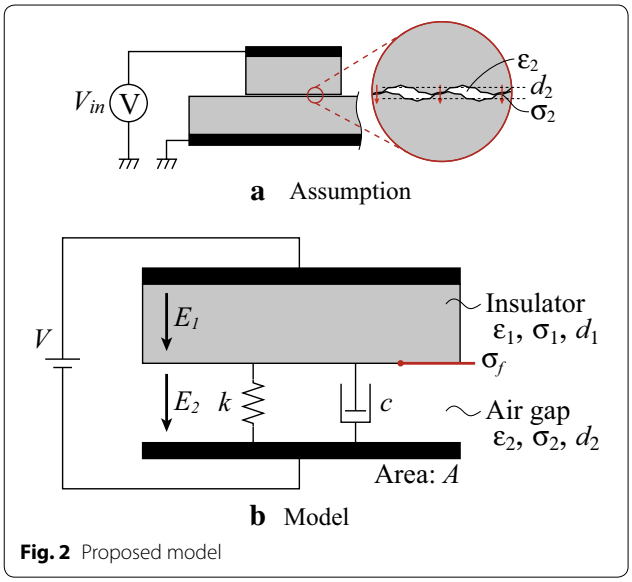

Fig. 2 Proposed model

The model consists of two dielectric layers: insulation layer and air-gap layer. Each layer, referred by index i ($i = 1$ insulation layer, 2 air-gap layer), has a uniform absolute permittivity ε_i, electrical conductivity σ_i, and thickness d_i. From the difference of the conductivity, interface charge σ_f accumulates at their interface, and thus the electric field of each layer, E_i, changes over time. Electroadhesion force, F_e, can be derived from the Maxwell stress of the air gap as

$$F_e = \frac{1}{2}\varepsilon_2 A E_2(t)^2, \tag{2}$$

where A is the area of the electrode. For ease of analysis, distortion of electric field at the edge of the plate is ignored.

Differential equation

First, we analyze the model under a constant gap, to verify that electric behavior of the model can describe the decrease of the electroadhesion force; the spring and the damper representing mechanical responses are ignored at this step. First, a differential equation for the electric field of the air gap is derived. Charge conservation at the interface provides

$$J_1 - J_2 = -\frac{\partial}{\partial t}(\varepsilon_1 E_1 - \varepsilon_2 E_2), \tag{3}$$

where J_i is the current density in each dielectric. Assuming Ohm's law, $J = \sigma E$, the above equation becomes

$$\sigma_1 E_1 - \sigma_2 E_2 = -\frac{\mathrm{d}}{\mathrm{d}t}(\varepsilon_1 E_1 - \varepsilon_2 E_2). \tag{4}$$

The boundary condition is expressed as

$$V = E_1 d_1 + E_2 d_2, \tag{5}$$

where V is the applied voltage. From Eqs. (4) and (5), the differential equation for E_2 is derived as

$$(\varepsilon_1 d_2 + \varepsilon_2 d_1)\frac{\mathrm{d}E_2}{\mathrm{d}t} + (\sigma_1 d_2 + \sigma_2 d_1)E_2 = \sigma_1 V + \varepsilon_1 \frac{\mathrm{d}V}{\mathrm{d}t}. \tag{6}$$

A symmetric equation can be derived for E_1.

DC behavior

Assuming that $V = V_0$ is applied during $t \geq 0$ and there is no initial charge at $t = 0$, Eq. (6) is solved as

$$E_2(t) = \frac{\sigma_1}{\sigma_1 d_2 + \sigma_2 d_1} V_0 \left(1 - e^{-\frac{t}{\tau}}\right) + \frac{\varepsilon_1}{\varepsilon_1 d_2 + \varepsilon_2 d_1} V_0 \, e^{-\frac{t}{\tau}}, \tag{7}$$

where τ is the time constant denoted as

$$\tau = \frac{\varepsilon_1 d_2 + \varepsilon_2 d_1}{\sigma_1 d_2 + \sigma_2 d_1}. \tag{8}$$

Equation (7) consists of two terms: incremental term related to the conductivities and decremental term related to the permittivity. When the former term is dominant, the resulting behavior becomes JR effect, where electroadhesion force gradually increases. On contrary, if the latter term becomes dominant, this model should be able to describe the force decreasing phenomenon reported in haptic studies.

The condition that defines the dominant term, can be obtained by calculating the interface charges. The interface charges, $\sigma_f(t)$, are calculated as

$$\begin{aligned} \sigma_f(t) &= -\varepsilon_1 E_1(t) + \varepsilon_2 E_2(t) \\ &= \frac{\sigma_1 \varepsilon_2 - \sigma_2 \varepsilon_1}{\sigma_1 d_2 + \sigma_2 d_1} V_0 \left(1 - e^{-\frac{t}{\tau}}\right). \end{aligned} \tag{9}$$

Depending on the sign of the numerator of the right-hand side of the equation, the interface charges become either negative or positive, as shown in Fig. 3 (the figure depicts $V_0 > 0$ condition). When the interface charges are negative, the field of the air gap, $E_2(t)$, decreases, which results in decrease of electroadhesion force, and vice versa. Therefore, the conditions for the two responses can be expressed as:

$$\begin{cases} \text{Force decrease: } \left(\frac{\varepsilon_1}{\sigma_1} > \frac{\varepsilon_2}{\sigma_2}\right), \\ \text{Force increase (JR effect): } \left(\frac{\varepsilon_1}{\sigma_1} < \frac{\varepsilon_2}{\sigma_2}\right). \end{cases} \tag{10}$$

It should be noted that the response considerably depends on the initial interface charges. If there are initial charges, $\sigma_f \neq 0$, at $t = 0$, the electric field changes as

$$E_2(t) = \frac{\sigma_1}{\sigma_1 d_2 + \sigma_2 d_1} V_0 \left(1 - e^{-\frac{t}{\tau}}\right) + \frac{\varepsilon_1 V_0 + \sigma_f(0) d_1}{\varepsilon_1 d_2 + \varepsilon_2 d_1} e^{-\frac{t}{\tau}}. \tag{11}$$

This clearly shows that the response of electroadhesion force, especially the second term, depends on the initial charge. It does not simply change the force response when voltage is applied. It also changes the response at voltage cut-off. When the voltage is turned off, the interface charges accumulated during the voltage application will cause residual adhesion force, as $V = 0$ does not result in zero field in the equation. Such residual force is well-known in Johnsen–Rahbek-type electrostatic chuck [20] and also observed in haptic devices [16, 22].

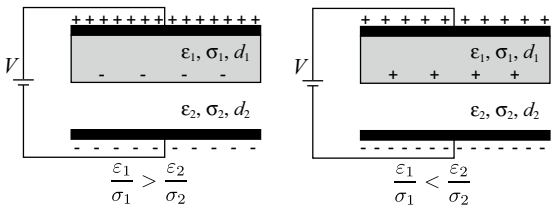

a Force decrease (decay) type **b** Johnsen-Rahbek type (Force increase)

Fig. 3 Physical meaning

AC behavior

When AC voltage, $V = V_0 \sin \omega t$, is applied and its frequency satisfies $\omega \gg \frac{1}{\tau}$, the electric field becomes

$$E_2(t) \approx \frac{\varepsilon_1}{\varepsilon_1 d_2 + \varepsilon_2 d_1} V_0 \, \sin \omega t, \tag{12}$$

which means interface charge does not accumulate in the AC case. As a result, the adhesion force is calculated as

$$F_e = \frac{1}{2} \varepsilon_2 A E_2(t)^2 = \frac{A}{2 \varepsilon_2 \left(\frac{d_1}{\varepsilon_1} + \frac{d_2}{\varepsilon_2}\right)^2} V^2 \tag{13}$$

This adhesion force equals to that calculated using the parallel plate model, Eq. (1), as $\varepsilon_2 = \varepsilon_0$.

Numerical simulation with mechanical response

In the actual systems, the air gap between the two plates fluctuates due to microscopic and/or macroscopic deformation of the electrodes. If the electroadhesion force changes rapidly, air damping by squeeze effect would also affect. In the proposed model, those gap variation is represented by the spring and the damper. The electroadhesion force compresses the air gap supported by the spring and the damper, and changes the air gap length, d_2, in the model.

The total response of the proposed model was numerically simulated as shown in Fig. 4, in comparison with the experimentally measured results which were obtained in the same setup as in [16]. It should be noted that the simulation results show the electroadhesion force whereas the experimental results show the friction force caused by electroadhesion. In the simulation, the electrical part was simulated using Eq. (6), and the mechanical part was simulated as a simple linear mass-spring-damper system. The simulation (a) utilized a high spring constant such that mechanical response can be ignored. On contrary, simulation (b) utilized a softer spring such that mechanical aspect becomes clear. Both simulation results successfully reproduced the force decay during constant voltage applications. However, simulation (a) failed to reproduce the initial response for the alternative pulse condition.

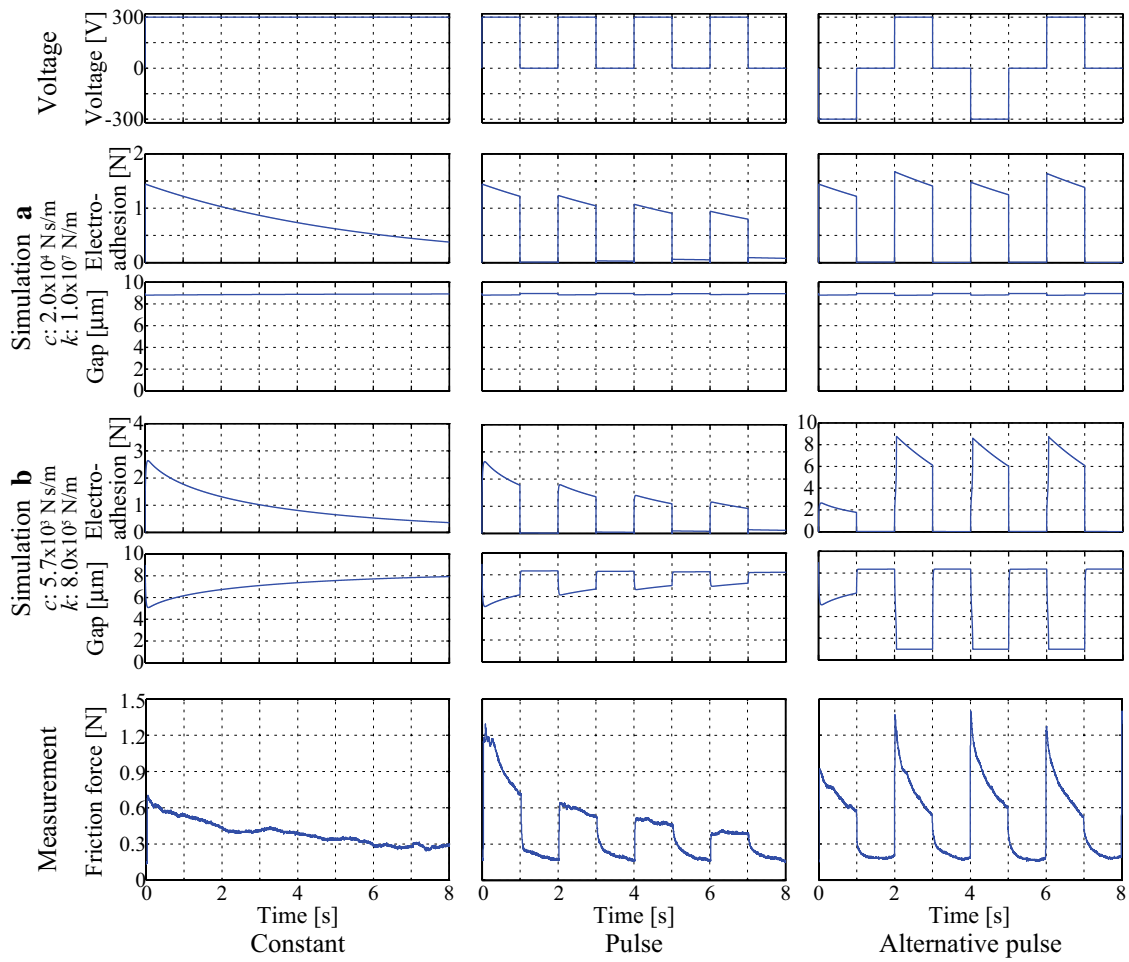

Fig. 4 Comparison of simulations (**a**, **b**) with friction force measurements. Simulation parameters are ε_1: 3.1 × ε_0 F/m, ε_2: 1.0 × ε_0 F/m, σ_1: 1.4 × 10^{-15} S/m, σ_2: 2.0 × 10^{-12} S/m, d_1: 16 μm d_2: 9 μm, (at $t = 0$), A: 7.1 × 10^{-4} m^2, and m (mass of layer 1): 1.0 × 10^{-3} kg

In the experiment, the response to the initial pulse was much smaller than the second and later responses. This was clearly reproduced in simulation (b). In the beginning, the gap was still large and the resulting force was small. However, during the first response, charges accumulated at the interface created large force at the second and later pulses. These results show the validity of the proposed model, as well as the benefit to combine mechanical response into JR model.

Control of electroadhesion

Concept

To control the electroadhesion force based on the proposed model, we need to derive the inverse model. First, the target field E is obtained as the inverse model of Eq. (2).

$$E = \sqrt{\frac{2}{\varepsilon_2 A}}\sqrt{F_e} \tag{14}$$

Then, the voltage that should be applied is obtained by solving Eq. (6). The Laplace transform of Eq. (6) is given as

$$\{(\varepsilon_1 d_2 + \varepsilon_2 d_1)s + (\sigma_1 d_2 + \sigma_2 d_1)\}\, E(s) = (\varepsilon_1 s + \sigma_1)\, V(s) \tag{15}$$

where $E(s)$ and $V(s)$ are Laplace transform of $E_2(t)$ and $V(t)$, respectively. By solving this equation in terms of $V(s)$, we obtain

$$V(s) = \frac{(\varepsilon_1 d_2 + \varepsilon_2 d_1)s + (\sigma_1 d_2 + \sigma_2 d_1)}{\varepsilon_1 s + \sigma_1}\, E(s). \tag{16}$$

Now, we need to think about the gap d_2. The gap is hidden and is normally in the order of micro meters, which can be hardly measured by using typical gap sensors. Therefore, when we apply this model to actual systems, we estimate the gap d_2 from the capacitance between two electrodes. As the relation between the gap and the capacitance is

$$C = \frac{A}{\frac{d_1}{\varepsilon_1} + \frac{d_2}{\varepsilon_2}}, \tag{17}$$

the gap, d_2, can be estimated from the measured capacitance as

$$d_2 = \varepsilon_2 \left(\frac{A}{C} - \frac{d_1}{\varepsilon_1} \right) \tag{18}$$

By substituting the estimated d_2 into Eq. (16), we can obtain the reference voltage that should reproduce the given force. It should be noted that, in this proposed control method, the spring and the damper in the electroadhesion model are not required, as the gap change is directly estimated by the gap sensor.

Experimental setup

In order to measure electroadhesion force continuously, indirect measurements through friction change were conducted. The measurement setup is shown in Fig. 5. The setup, which is basically the same as the one used in [18], consists of a voltage source, a pad, a motorized stage, a built-in gap (capacitance) sensor, and a loadcell for evaluation. The pad (30 mm in diameter and 7 mm in thickness), which was fabricated using a 3D printer, was made of ABS resin. The bottom surface of the pad was covered by a 1-mm-thick silicone rubber sheet and then by a 9-μm-thick PET (polyethylene terephthalate) sheet. The PET sheet had a deposited aluminum layer on its top surface (it should be noted that the bottom surface of the PET sheet touched the stage, which means the aluminum electrode was covered by an insulating PET layer). The stage was a metal plate (stainless steel) whose top surface was covered by an adhesive PET sheet (Kimoto, PA-8X, 8 μm in thickness) for insulation. While a voltage for electroadhesion was applied between the pad electrode and the stage, the pad was horizontally pushed against the loadcell by the motorized stage, such that the loadcell could measure friction change as the electroadhesion response. The built-in sensor estimated the gap fluctuation through capacitance measurement.

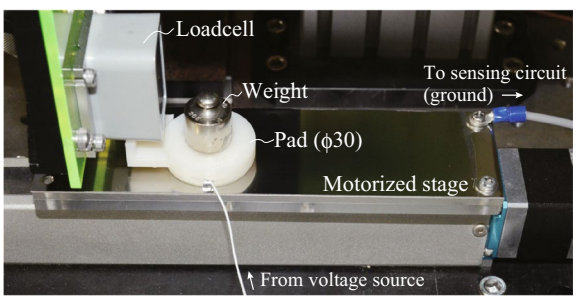

Fig. 5 Experimental setup

Neutralizing method

In preliminary measurements, we found that the responses of the electroadhesion force was not stable. This would be due to the initial surface charges, as explained in the model. To obtain reproducible results, the initial charges must be neutralized before the experiments.

For neutralization, we tested four different protocols. The first two protocols utilized an ionizer, as shown in Fig. 6(i). The ionizer (SUNX, ER-F12) was arranged above the setup and was activated for 2 min for protocol (a), and 15 min for (b). In the protocol (c), we combined the ionizer and ethanol. After neutralizing surface charges using the ionizer, we gently wiped the surface using a cleaning paper (OZU co., BEMCOT PS-2) impregnated with ethanol as shown in Fig. 6(ii). The protocol (d) only utilized a cleaning paper with ethanol; we rubbed the surface by the cleaning paper.

The results of force measurement to confirm the effect of the neutralizations are shown in Fig. 7. The surface of the setup has been neutralized by the four protocols, four times each. After the neutralization, voltage was applied and electroadhesion force was measured by moving the stage. The protocols (a), (b), and (d) showed unstable responses; the force variations are different among trials. In the protocol (c), on contrary, the force response was stable; it showed the same curve for four trials. Although it is not shown in the figure, we also tested gentle wipe using a cleaning paper with ethanol (without using ionizer) that also showed unstable responses. These results show that the combination of an ionizer and cleaning paper with ethanol can effectively remove the surface charges.

In these results, protocol (d) showed larger friction force than other protocols. This would be probably because ethanol affected the surface treatment of the film. This suggests that the use of ethanol should be minimized to prevent surface damage.

Calibration

After neutralizing the surface charge, a step response of the friction force against a step voltage input was

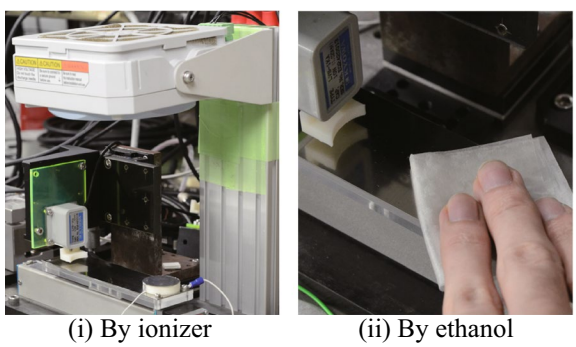

(i) By ionizer (ii) By ethanol

Fig. 6 Appearance of neutralizing

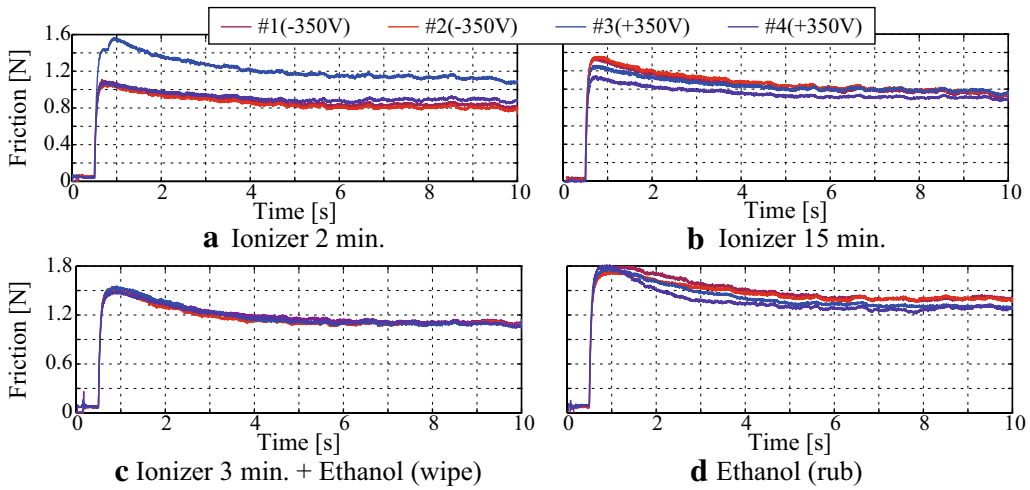

Fig. 7 Results of neutralizing

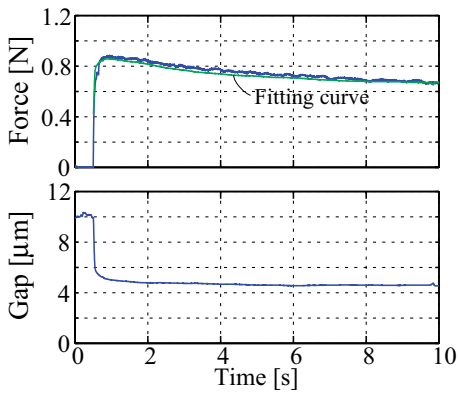

Fig. 8 Results of calibration

measured on the stage moving at a constant speed (4 mm/s). The gap variation was measured at the same time using the gap sensor. The results are shown in Fig. 8. From these plots, conductivities, σ_1, σ_2 and friction index μ were manually obtained, such that the model could produce the obtained force variation under the measured gap variation. The relative permittivity of the air was assumed to be 1.0, whereas that of the insulating film was set as 3.1, which is a typical value for PET film.

Control of dynamic response

Using the calibrated parameters, force control experiments have been carried out. The temperature was between 18 and 26 °C and relative humidity was between 15 and 30%. The results are shown in Fig. 9. The two columns show two different control methods. The first control method on the left column, which is denoted as "PP model", utilized the parallel-plate capacitance model as described in Eq. (1). In this method, the gap was assumed constant and the applied voltage was determined by solving Eq. (1) under a constant gap. In the other method on the right column, which is referred to as "Proposed model", the gap was estimated from the gap (capacitance) sensor [18] and the voltage was obtained by using Eqs. (14) and (16).

In plots (a) and (b), the force decay that appeared in PP model was successfully compensated by using the proposed model. As shown in plot (c), PP model showed residual force after cutting off the voltage. On the other hand, in the proposed model, the voltage was not totally cut but was kept at some small value, which resulted in zero residual force. In plot (d), responses against polarity-alternating pulses are shown. Although the proposed model showed far improved responses compared to the conventional PP model, the response against the negative pulse showed some deviation. This would be because the model parameters (σ_i) were identified for a positive voltage. For better force control, a better parameter identification method needs to be investigated.

Discussions

The model proposed in this paper did not consider the relative motion of the electrodes, although the electrodes were moving during the experiments. In [27], it has been reported that the electrode motion affected the adhesion force. Since their electrodes were inter-digital electrodes, their results cannot immediately apply to our system. However, their results suggest that the adhesion force would change also in our system. In our system, if the electrodes relatively move, the charges at their interface, σ_f, would virtually reduce, as the facing areas will be continuously changing. In other words, the charges accumulated on the stage surface will be left behind

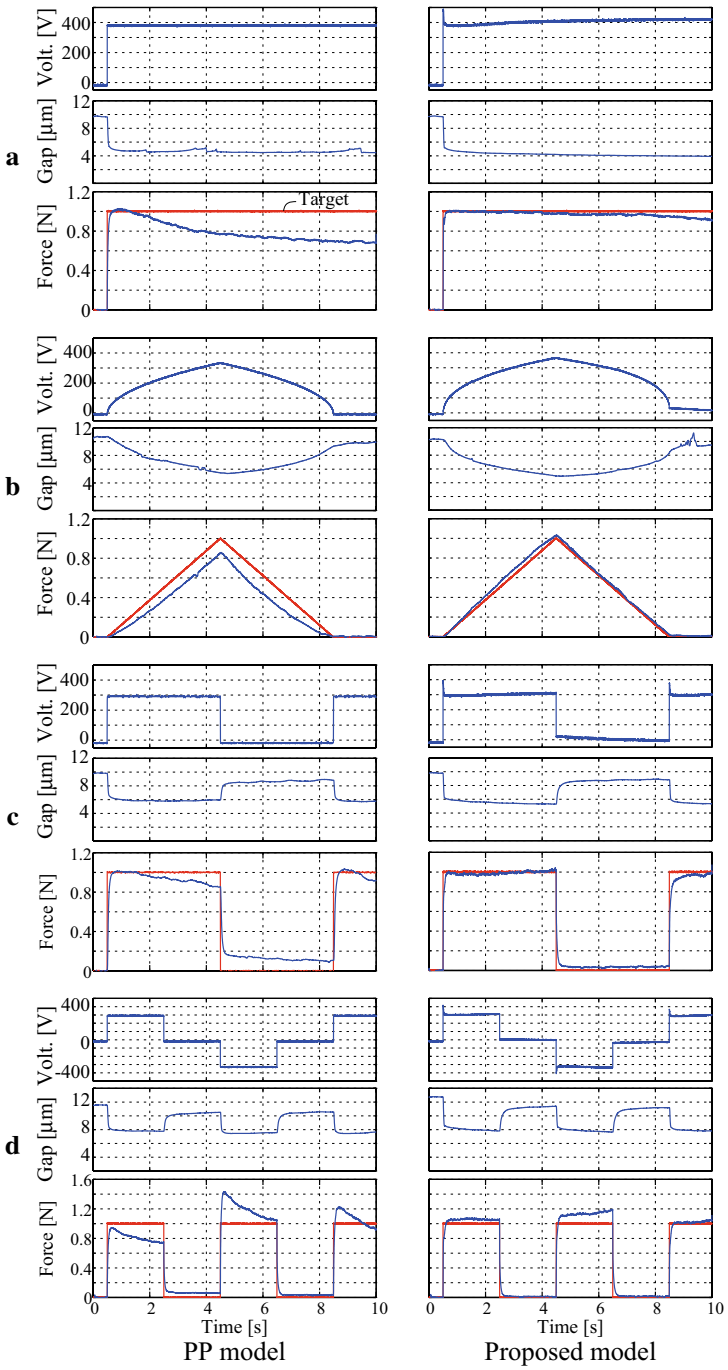

Fig. 9 Results of the force control

as the pad moves. The newly facing part does not have accumulated charge, which virtually decreases the interface charge, σ_f.

In the experiments of this work, this effect was negligible, as the parameter identification and control experiments were all carried out at the same speed. However, to cope with various motion speeds, the model needs some modifications such that it can account for the virtual charge decrease due to the relative motions.

The voltages used in the experiments were limited to ±500 V, and most of the measurements were carried out at around 300–400 V. This voltage range is typical (or

slightly higher) for haptic applications. For robotic applications, however, much higher voltages, such as several kilo volts, are often utilized. It has been experimentally shown that the electroadhesion force does not follow the square relationship in such a higher voltage range [8]. Therefore, it should be verified in future work if the proposed model is valid in higher voltage ranges.

It has also been known that humidity affects the performance of electroadhesion [28, 29]. This would be because the humidity affects the conductivity of the air gap (and the surface insulator). In the proposed model, if we assume very high conductivity for the air gap, the resulting electroadhesion force vanishes instantly, which corresponds to the observation in [28]. Such an aspect of the proposed model also needs to be further investigated in future work.

Conclusion

This paper proposed an electro-mechanical combined model for electroadhesion, which consists of an insulator and an air gap, and realized electroadhesion force control in DC voltage, which was found difficult in the previous studies. The electrical part of the model is based on the JR model, in which interface charges accumulate under a DC voltage. By considering the sign of the surface charges, the model can explain force decrease, which has been observed in haptic device applications. The mechanical part simulates fluctuation of the air gap, which affects the dynamic response, since the force magnitude and the time constant depend on the gap. The numerical simulations using the combined model successfully reproduced the characteristic behaviors of electroadhesion force. It was also shown that the initial response of the electroadhesion force can be reproduced only when mechanical part is actively involved. Using the inverse of the proposed model, as well as a built-in capacitive-type gap sensor, experiments to control dynamic force response were carried out. The experimental results verified that the proposed method can suppress errors due to characteristic behaviors of electroadhesion. This work also revealed the importance of surface-charge neutralization for reproducible responses of electroadhesion. These knowledges would contribute to better understanding and controlling of electroadhesion systems, especially for haptic and robotic applications.

Authors' contributions

TN contributed to the modeling, analysis, experiments, and drafting of the manuscript. AY took part in the modeling, interpretation of data, and revising of the manuscript. Both authors read and approved the final manuscript.

Acknowledgements

Not applicable.

Competing interests

Both authors declare that they have no competing interests.

Availability of data and materials

The datasets supporting the conclusions of this article are included within the article.

Funding

This work was supported in part by Grant-in-Aid for JSPS Fellows (No. 269272) and Grand-in-Aid for Scientific Research (B) (No. 26280069) from JSPS, Japan.

Publisher's Note

Received: 9 April 2017 Accepted: 6 June 2017
Published online: 14 June 2017

References

1. Wardly GA (1973) Electrostatic wafer chuck for electron beam microfabrication. Rev Sci Instrum 44(10):1506–1509
2. McGinty GK (1976) Semiconductor device manufacture. US Patent 3,993,509
3. Graule MA, Chirarattananon P, Fuller SB, Jafferis NT, Ma KY, Spenko M, Kornbluh R, Wood RJ (2016) Perching and takeoff of a robotic insect on overhangs using switchable electrostatic adhesion. Science 352(6288):978–982. doi:10.1126/science.aaf1092
4. Shintake J, Rosset S, Schubert B, Floreano D, Shea H (2016) Versatile soft grippers with intrinsic electroadhesion based on multifunctional polymer actuators. Adv Mater 28(2):231–238
5. Yamamoto A, Nakashima T, Higuchi T (2007) Wall climbing mechanisms using electrostatic attraction generated by flexible electrodes. In: IEEE international symposium on micro-nano mechatronics and human science, 2007. MHS'07. pp 389–394
6. Prahlad H, Pelrine R, Stanford S, Marlow J, Kornbluh R (2008) Electroadhesive robots—wall climbing robots enabled by a novel, robust, and electrically controllable adhesion technology. In: IEEE international conference on robotics and automation, 2008. ICRA 2008. pp 3028–3033
7. Wang H, Yamamoto A, Higuchi T (2014) A crawler climbing robot integrating electroadhesion and electrostatic actuation. Int J Adv Robot Syst 11:191
8. Koh KH, Sreekumar M, Ponnambalam SG (2014) Experimental investigation of the effect of the driving voltage of an electroadhesion actuator. Materials 7:4963–4981
9. Mao J-B, Qin L, Zhang W-X, Xie L, Wang Y (2015) Modeling and analysis of electrostatic adhesion force for climbing robot on dielectric wall materials. Eur Phys J Appl Phys 69(1):11003
10. Guo J, Justham L, Jackson M, Parkin R (2015) A concept selection method for designing climbing robots. Key Eng Mater 649:22–29
11. Chen R, Huang Y, Tang Q (2017) An analytical model for electrostatic adhesive dynamics on dielectric sustrates. J Adhes Sci Technol 31(11):1229–1250
12. Bamber T, Guo J, Singh J, Bigharaz M, Petzing J, Bingham PA, Justham L, Penders J, Jackson M (2017) Visualization methods for understanding the dynamic electroadhesion phenomenon. J Phys D Appl Phys 50:205304
13. Yamamoto A, Nagasawa S, Yamamoto H, Higuchi T (2006) Electrostatic tactile display with thin film slider and its application to tactile telepresentation systems. IEEE Trans Vis Comput Graph 12(2):168–177
14. Bau O, Poupyrev I, Israr A, Harrison C (2010) Teslatouch: electrovibration for touch surfaces. In: Proceedings of the 23rd annual ACM symposium on user interface software and technology. UIST '10. pp 283–292
15. Linjama J, Mäkinen V (2009) E-sense screen: novel haptic display with capacitive electrosensory interface. Presented at HAID 09, 4th workshop for Haptic and audio interaction design, Dresden, Germany
16. Nakamura T, Yamamoto A (2013) Multi-finger electrostatic passive haptic feedback on a visual display. In: IEEE world haptics conference (WHC), 2013. pp 37–42

17. Nakamura T, Yamamoto A (2016) A multi-user surface visuo-haptic display using electrostatic frcition modulation and capacitive-type position sensing. Trans Haptics 9(3):311–322
18. Nakamura T, Yamamoto A (2016) Interaction force estimation on a built-in position sensor for an electrostatic visuo-haptic display. ROBOMECH J 3(11):1–11
19. Watanabe T, Kitabayashi T, Nakayama C (1993) Relationship between electrical resistivity and electrostatic force of alumina electrostatic chuck. Jpn J Appl Phys 32(2R):864
20. Kanno S, Usui T (2003) Generation mechanism of residual clamping force in a bipolar electrostatic chuck. J Vac Sci Technol B 21(6):2371–2377
21. Kanno S, Kato K, Yoshioka K, Nishino R, Tsubone T (2006) Prediction of clamping pressure in a Johnsen–Rahbek-type electrostatic chuck based on circuit simulation. J Vac Sci Technol B 24(1):216–223
22. Giraud F, Amberg M, Lemaire-Semail B (2013) Merging two tactile stimulation principles: electrovibration and squeeze film effect. In: World haptics conference (WHC), 2013. pp 199–203
23. Strong RM, Troxel DE (1970) An electrotactile display. IEEE Trans Man Mach Syst 11(1):72–79
24. Meyer DJ, Peshkin MA, Colgate JE (2013) Fingertip friction modulation due to electrostatic attraction. In: World haptics conference (WHC), 2013. pp 43–48
25. Vezzoli E, Amberg M, Giraud F, Lemaire-Semail B (2014) Electrovibration modeling analysis. In: Haptics: neuroscience, devices, modeling, and applications. Springer, Berlin, pp 369–376
26. Johnsen A, Rahbek K (1923) A physical phonomenon and its applications to telegraphy, telephony, etc. J Inst Electr Eng 61(320):713–725
27. Chen R, Huang Y, Tang Q, Bai L (2016) Modelling and analysis of the electrostatic adhesion performance considering a rotary disturbance between the electrode panel and the attachment substrate. J Adhes Sci Technol 30(21):2301–2315
28. Tang H, Beebe DJ (1998) A microfabricated electrostatic haptic display for persons with visual impairments. IEEE Trans Rehabil Eng 6(3):241–248
29. Guo J, Bamber T, Chamberlain M, Justham L, Jackson M (2016) Optimization and experimental verification of coplanar interdigital electroadhesives. J Phys D Appl Phys 49:415304